



## Distribution of nanoparticle depositions after a single breathing in a murine pulmonary acinus model



Toshihiro Sera<sup>a,\*</sup>, Ryosuke Higashi<sup>b</sup>, Hisashi Naito<sup>b</sup>, Takeshi Matsumoto<sup>b</sup>, Masao Tanaka<sup>b</sup>

<sup>a</sup> Department of Mechanical Engineering, Kyushu University, 744 Motoooka, Nishi-ku, Fukuoka 819-0395, Japan

<sup>b</sup> Department of Mechanical Science and Bioengineering, Graduate School of Engineering Science, Osaka University, 1-3, Machikaneyama, Toyonaka, Osaka 560-8531, Japan

### ARTICLE INFO

#### Article history:

Received 3 June 2016

Received in revised form 9 November 2016

Accepted 19 December 2016

Available online 1 January 2017

#### Keywords:

Computational fluid dynamics

Particle deposition

Pulmonary acinus

Synchrotron radiation-CT

Acinar generation

### ABSTRACT

We quantitatively investigated nanoparticle deposition (density:  $1.0 \text{ g/cm}^3$ , diameter:  $0.1\text{--}1.0 \text{ }\mu\text{m}$ ) in a pulmonary acinus using computational fluid dynamics. We assumed that acinar flow was induced by the expansion and contraction of the acinar model, with the volume changing sinusoidally with time as the boundary condition. We based the complicated acinar model and volume change on a mammalian lung, and evaluated the distribution of particle depositions through acinar generation based on three dimensional thinning. The maximum Reynolds numbers at the inlet and terminal alveoli were 0.191 and  $1.93 \times 10^{-3}$ , respectively. With only gravitational force, particle deposition was strongly affected, except for the  $0.1\text{-}$  and  $0.2\text{-}\mu\text{m}$  particles, and the  $0.8\text{-}$  and  $1.0\text{-}\mu\text{m}$  particles were deposited around the inlet due to sedimentation after the beginning of inflation. We found that the  $0.1\text{-}$  to  $0.4\text{-}\mu\text{m}$  particles were deposited at the distal alveoli and that the deposition was enhanced by both the gravitational and Brownian forces, despite the small terminal velocity. For the  $0.1\text{-}$  and  $0.2\text{-}\mu\text{m}$  particles in particular, the particles were deposited throughout the acinus. The maximum deposition fraction of each acinar segment reached 1.2% after a single breath, and was higher in the middle generations and at the terminal alveoli.

© 2016 Elsevier Ltd. All rights reserved.

## 1. Introduction

The estimation of particle deposition in the lungs is a key factor in any evaluation of the effectiveness of inhaled pharmacological agents and the toxic effects of pollutant particles. The appropriate amount of aerosol that should be deposited at the appropriate sites at specific depths in the lung so as to maximise the drug's effects and to minimise its side effects. The particle deposition has been studied using simple bifurcation model [1–4] and image-based realistic airway model [5,6]. Kleinstreuer et al. proposed the new methodology for optimal drug-aerosol delivery and simulated the micron particle trajectories using human oral airway model with tracheobronchial airways [7]. Xi and Longest develops the correlation of particle deposition for both inertial and diffusive transport by drift flux model with a near-wall velocity correction, and evaluated the transport and deposition of submicrometer aerosols in the nasal cavity [8]. According to a previous report, inhaled particles greater than  $6 \text{ }\mu\text{m}$  in diameter are mainly filtered in the upper airways; therefore, it is primarily smaller particles with a diameter of less than  $2 \text{ }\mu\text{m}$  that are able to reach the alveolar region [9]. van

Ertbruggen et al. experimentally measured flow structures in a three-dimensional (3D) scaled-up model of an alveolated bend with rigid walls [10]. Darquenne et al. measured the deposition of aerosolised  $0.95\text{-}\mu\text{m}$ -diameter ferric oxide particles using a 3T magnetic resonance imaging (MRI) in order to investigate the effect of gravity on the peripheral deposition of fine particles [11]. Fishler and Sznitman fabricated an acinar-like microfluidic model and measured the acinar flow and particle deposition [12,13]. However, it is still difficult to create a complex acinar model and to visualise particle deposition in great detail *in vivo* for evaluating of particle deposition. Therefore, a numerical simulation method is very useful for investigating aerosol particles in the alveolar region.

Several researchers have investigated flow phenomena and particle transport in an idealised pulmonary alveolar duct model using numerical simulation. Tsuda et al. generated a two-dimensional (2D) central thoroughfare channel surrounded by a torus as the pulmonary duct, and examined the effects of the rhythmical expansion and contraction of breathing in a sinusoidal manner [14]. Haber et al. extended this 2D model to a 3D model and investigated gravitational particle deposition with rhythmical airway motion [15]. Alveolar flow and particle deposition have also been simulated in 3D simple alveolar ducts, such as a cylindrical channel

\* Corresponding author.

E-mail address: [sera@mech.kyushu-u.ac.jp](mailto:sera@mech.kyushu-u.ac.jp) (T. Sera).

mounted with an isolated spherical cavity [16], a fully alveolated duct [17], and assemblages of polyhedra forming a space-filling asymmetrical acinar branching tree [18]. According to these computational simulations using the moving boundary problem, the alveolar flows induced by rhythmical airway motion were kinematically irreversible and dominated by recirculating and radial flows, in contrast to the rigid alveoli model [19]. Tsuda et al. observed the flow patterns in fresh excised lungs and found that low-Reynolds-number acinar flow was neither simple nor reversible [20]. Ma et al. developed a multigenerational 3D idealised model of alveolated airways with arbitrary bifurcation angles and a spherical alveolar shape, and simulated the deposition of 1- and 3- $\mu\text{m}$  aerosol particles [21].

The pulmonary acinus is defined functionally as the largest lung unit in which all airways participate in gas exchange, and anatomically consists of an asymmetrical branched series of alveolar ducts, associated surrounding alveoli, and groups of alveolar sacs originating from a terminal bronchiole. As we mentioned above, in the previous studies, an idealised pulmonary alveolar duct model was used for flow phenomena and particle transport in acinar region. However, the aerosol deposition efficiency in deep regions of the lung can be influenced by complex pulmonary geometry. Sera et al. simulated micro-particle deposition (diameters 1 and 3  $\mu\text{m}$ ) in a pulmonary acinar model based on high-resolution, synchrotron-based computed tomography (CT) of a mammalian lung [22]. That study focused mainly on the effect of complex geometry on micro-particle deposition and the effect of gravity orientation on particle transport and deposition. Additionally, the deposition efficiency was only evaluated macroscopically and qualitatively. However, nano-particles also play an important role in particle deposition in the acinar region. In this study, therefore, we investigated the quantitative distribution of nanoparticle deposition (diameters 0.1–1.0  $\mu\text{m}$ ) in a complex realistic acinar model based on synchrotron CT images of a mammalian lung. To estimate the particle deposition quantitatively in the acinar region after a single breath, the particle deposition fraction was evaluated via acinar generation defined using a 3D skeleton of the acinar model. We assumed that acinar flow was induced by self-similar expansion and contraction in a sinusoidal manner, and focused on the drag force, gravitational force, and Brownian force acting on the particles. Our previous study showed that the transport of 1.0- $\mu\text{m}$  particles in the acinus was affected by gravity [22]. Tsuda et al. estimated that the diffusion distance of 0.1- $\mu\text{m}$  particles for 1.0 s was approximately 25  $\mu\text{m}$ , suggesting that the Brownian force may affect the aerosol deposition [23] because the alveolar diameter is approximately 100  $\mu\text{m}$  [22].

## 2. Methods

### 2.1. Pulmonary acinar model

The pulmonary acinar model was based on CT images of a closed-chest mouse (A/J, 9 weeks) [24]. All experimental protocols were approved by the SPring-8 Experimental Animals Care and Use Committee. SPring-8 is a third-generation synchrotron radiation source in Hyogo, Japan, and offers a higher-flux X-ray than a laboratory X-ray source, resulting in higher contrast resolution. The isotopic voxel size was 2.8  $\mu\text{m}$ . In this study, the acinus model was reconstructed from synchrotron CT images at functional residual capacity (FRC). FRC was defined as the lung volume at euthanasia, and the lung airway pressure was 0 cm H<sub>2</sub>O. In addition, to estimate the acinar volume change after inflation, the same acinus was imaged at total lung capacity (TLC) [24]. The catheter was fastened using a suture and the junction was fixed in place using cyanoacrylate instant adhesive to prevent an air leak. TLC was

defined as the lung volume at 1.0-ml air inflation and a pressure of 25.0 cm H<sub>2</sub>O. After CT imaging, we identified cross-sections of the same acinus at FRC and TLC using a threshold-based 3D region-growing algorithm. After segmentation, false holes were sealed by manually adding voxels to the surface of the parenchyma. Finally, the connectivity of the segmented acinus with a resolution of less than  $500 \times 500 \times 500$  pixels was checked manually. The acinar volumes at FRC and TLC ( $V_{\text{FRC}}$  and  $V_{\text{TLC}}$ ) were calculated as the number of voxels multiplied by the volume of a single voxel.

Fig. 1(A) depicts the murine pulmonary acinar models reconstructed from segmented CT images. The diameters of alveolar ducts and alveoli ranged approximately 40–100  $\mu\text{m}$  and 30–60  $\mu\text{m}$ , respectively. To avoid any boundary condition influence and to achieve fully developed inflow at the inlet of the acinus with a diameter of 80  $\mu\text{m}$ , the inlet was artificially lengthened with a straight tube in the direction of the skeleton, as calculated by a 3D thinning algorithm (Amira software, Visage Imaging, Germany). This algorithm performs a Euclidean distance (the distance from the background) transformation and repeatedly checks that the Euclidean distance value is small as the voxels are deleted in

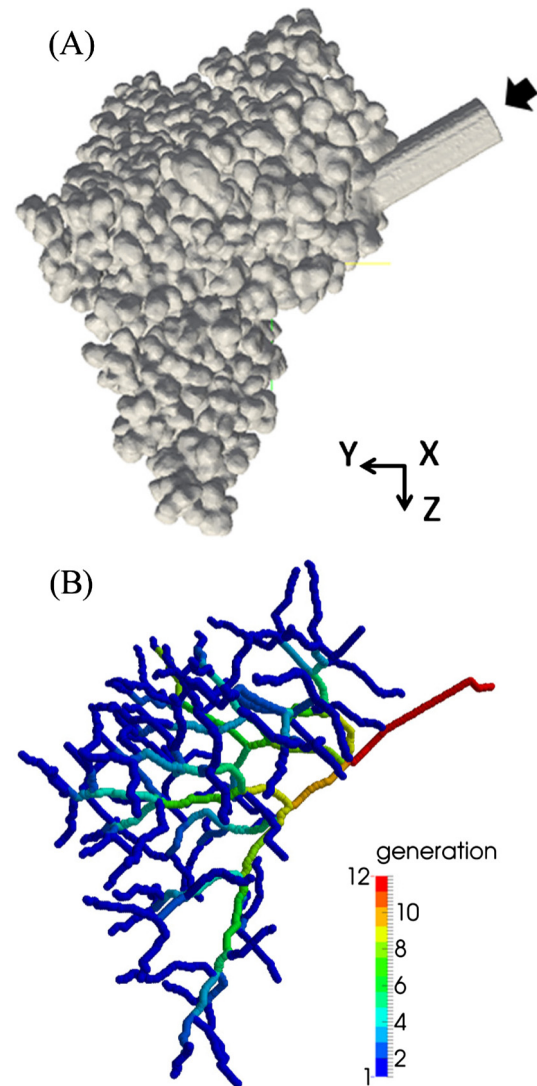


**Fig. 1.** The acinar model based on (A) synchrotron CT images and (B) acinar generation. To avoid any influence of the boundary conditions on the computer simulation, the inlet indicated by the arrow was artificially lengthened using a straight tube 80  $\mu\text{m}$  in diameter (A). The “generation” of the terminal alveoli was 1 and that of the inlet was 12 (B).

Download English Version:

<https://daneshyari.com/en/article/4994314>

Download Persian Version:

<https://daneshyari.com/article/4994314>

[Daneshyari.com](https://daneshyari.com)